

## Performance Analysis of Duct Vane Application on Patrol Boats Using Computational Fluid Dynamics

Muhammad Arif Budiyanto<sup>1\*</sup>, Fadhil Naufal<sup>1</sup>, Gerry Liston Putra<sup>1</sup>, Acmad Riadi<sup>2</sup>,  
Dedy Triawan Suprayogi<sup>2</sup>, Muhammad Iqbal<sup>3</sup>, Triwilaswandio Wuruk Pribadi<sup>4</sup>

<sup>1</sup>Naval Architecture and Marine Engineering, Department of Mechanical Engineering, Universitas Indonesia, Depok, West Java, 16424, Indonesia

<sup>2</sup>Department of Mechanical Engineering, Universitas Sultan Ageng Tirtayasa, 42435, Indonesia

<sup>3</sup>Naval Architecture, Ocean and Marine Engineering, University of Strathclyde, Glasgow, Scotland, SC015263

<sup>4</sup>Department of Naval Architecture and Marine Engineering, Institut Teknologi Sepuluh Nopember, 60111, Indonesia

**Abstract.** Fast patrol boats are designed for high performance in surveillance and warfare missions. In terms of hull technology development, the fast patrol boat commonly uses a V-type hull with hard chine. A duct vane is an innovation developed to improve the performance of patrol boats by combining the principles of wake-equalizing duct and hydrofoil. The objective of this paper is to investigate the hydrodynamic effect of the application of duct vane on the patrol boat hull design. The investigation was carried out using computational fluid dynamics that was validated using experiment data. The result of the duct vane application can improve the ship speed performance and reduce the total resistance by 40% at  $F_n$  0.6. The results of this study also provide an overview of the influence of the duct vane on the lift force of a hard chine hull-type.

**Keywords:** Duct vane; Hydrodynamics; Patrol boat

### 1. Introduction

The wake equalizing duct (WED) is a component that can improve the ship's propulsion system and the economic performance of the ship (Furcas *et al.*, 2020). WED component consists of two semicircular duct airfoil nozzles, which are mounted in two sections at the rear of the ship and in front of the propeller (Korkut, 2006). In that section, the duct accelerates the flow to the top of the propeller while slightly slowing it down to the bottom of the propeller, thereby generating a more homogeneous wakefield. WED can make the flow through the duct accelerate faster towards the top of the propeller while maintaining a relatively slower flow at the bottom of the propeller (Go, Yoon, and Jung, 2017). WED is able to make the flow more uniform so that there is no separation at the rear of the ship (Seo, Yoon, and Kim, 2022). The incorporation of WED has the capability to enhance propeller thrust and minimize excitation vibrations. This is achieved by ensuring a uniform and homogeneous flow to the propeller, consequently reducing propeller excitation vibrations (Rezaei, Bamdadinejad, and Ghassemi, 2022). In addition to increasing the

---

\*Corresponding author's email: [ma.budiyanto@ui.ac.id](mailto:ma.budiyanto@ui.ac.id), Tel.: +6282113942255  
doi: [10.14716/ijtech.v15i2.6661](https://doi.org/10.14716/ijtech.v15i2.6661)

performance of the propulsion system, WED also increases the performance of the steering system on ships (Çelik, 2007).

Based on experiments regarding the effect of using WED on ship resistance, propulsion performance, and visualization of flow at the rear of the ship, it is illustrated that the flow that occurs in ships that have been optimized with WED has a more homogeneous flow compared to the original ship shape (Tacar *et al.*, 2020). Flow characteristics pass through the rear of the original ship shape, with the rear being optimized with WED (Tacar *et al.*, 2020). The results show that the shape of the ship that has been optimized using WED can reduce resistance compared to the original shape of the ship. This reduction in resistance occurs due to a reduction in the separation of the boundary layer (Wu, Chang, and Huang, 2022).

Several researchers use computational fluid dynamics for ship resistance investigation. The excellent agreement between model testing and CFD predictions for total ship resistance in calm water has resulted in a high confidence level in the CFD results (Riyadi, Aryawan, and Utama, 2022). The total resistance and increased resistance caused by the hydroelastic body were explored, as well as the hydroelastic body's influence on the magnitude of resistance and added resistance (Baso *et al.*, 2022). Actively reducing ship resistance can have an effect when considering the ship energy efficiency management plan (Dawangi and Budiyanto, 2021).

The increase in ship propulsion performance is also due to the reduced number of flow separations at the rear (Kim and Kinnas, 2022). The flow at the back tends to be more homogeneous, resulting in a reduction in required power. However, a significant challenge in high-speed propellers remains cavitation (Duy *et al.*, 2022; Köksal *et al.*, 2021). Cavitation is defined as the process of forming a liquid vapor phase due to reduced pressure at a constant room temperature (Yusvika *et al.*, 2020). The process occurs more because of the decrease in pressure than the addition of heat. Cavitation in the propeller occurs in the part of the propeller that has low pressure which is at the top of the propeller. At this time, the fluid phase change began to occur from liquid fluid to vapor fluid. This form of cavitation is in the form of air bubbles (Köksal *et al.*, 2021).

Duct vane is an innovation that can be used for fast patrol boats. This innovation combines the principle of a wake equalizing duct with a hydrofoil (Budiyanto, Syahrudin and Murdianto, 2020). The wake equalizing duct is a component that can increase the propulsion performance of the ship (Syahrudin, Budiyanto, and Murdianto, 2020). This component consists of two duct foil nozzles in the shape of a semicircle which are installed in two parts behind the ship and in front of the propeller (Budiyanto, Murdianto, and Syahrudin, 2020a). This component works by directing the fluid flow to the top of the propeller to increase the speed of the thrust force on the ship using the hydrofoil concept (Budiyanto, Murdianto, and Syahrudin, 2020a). The hydrofoil works by utilizing the speed of the ship so that it can lift the hull out above the water surface where the hull is not subject to frictional resistance by the water fluid (Daskovsky, 2000).

The objective of this paper is to investigate the application of duct vane on patrol boats by the simulation model. The investigation includes the hydrodynamic parameters, such as a comparison of drag coefficient and lift force analysis. The originality of this study is the use of a hard-chine hull for the basic design of patrol boats. The contribution of this study is twofold: first, to offer an overview of the effect of duct vane on hydrodynamic parameters, and second, to present the advantages associated with the application of duct vane on patrol boats. The hydrodynamic characteristics of the duct vane used by patrol boats are investigated to find the resistance of the ship using a computational fluid dynamics simulation method so that it becomes the basis for considering the use of duct vanes on fast

patrol boats. The independent variable in this study is the speed of the water flow. The examination of these variables allows us to understand the impact of water flow speed on the resulting hydrodynamic parameters.

## 2. Material Method

### 2.1. Design and the Principal Dimension of the Patrol Boat

A fast patrol boat using a hard-chine hull with a duct vane is designed using linear algebra to determine the meeting points of the plates so that the coordinates are in one flat plane on each plate. The line plan is made into a 3D model using Maxsurf UK ([Maxsurf, n.d.](#)). The ship design employed in this study is a model characterized by main dimensions, including a length overall of 0.75 m, breadth of 0.2 m, height of 0.12 m, and draught of 0.049 m.

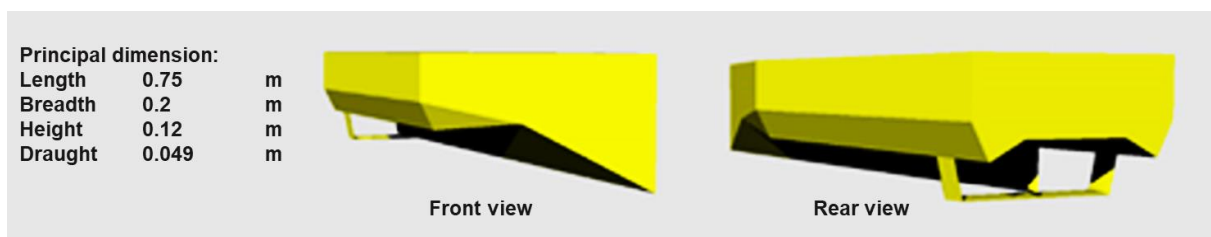


**Figure 1** Fast patrol boat design with flat plate hull with duct vane

In calculating the need for Hydrofoil on the Duct Vane, the Hydrofoil lift calculation formula is used on the ship by using Equation 1 ([Vellinga, 2009](#)). Where  $L$  = Lift force (N),  $A$  = projected surface area ( $m^2$ ),  $V$  = speed (m/s),  $C_L$  = coefficient of lift, and  $F_{AR}$  = factor correction for aspect ratio.

$$L = V^2 \times A \times C_L \times F_{AR} \quad (1)$$

Each profile of the hydrofoil section has its own coefficient of displacement depending on the characteristics of the profile shape. After determining the profile used, the next step is to calculate the lift using Equation 1. Through the results of the calculation of the lift from the hydrofoil, the area of the duct vane is obtained, as well as the shape of the hydrofoil used in the duct vane. The profile used for the duct vane is NACA 4412 ([AirfoilTools.com, n.d.](#)), and the shape of the hydrofoil used on the duct vane is shown in Figure 2. Detail information of the foil used on the duct vane are Profile NACA 4412, Span 0.2064 m, Chord 0.027821 m, Area 0.0078674  $m^2$ ,  $F_{AR}$  0.67,  $C_L$  0.4 and Lift 19.76 N.

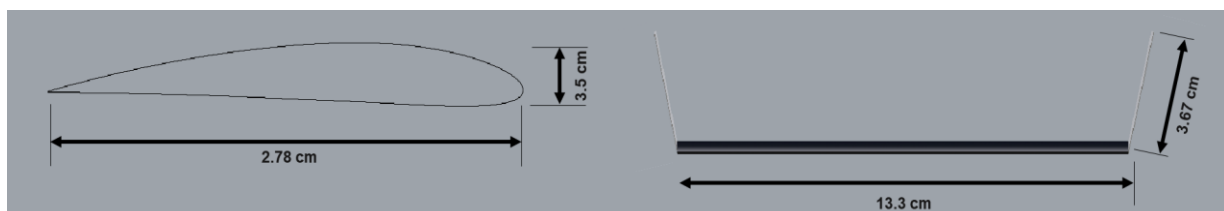


**Figure 2** Cross section of NACA 4412 used as hydrofoil

### 2.2. Simulation Setting and Parameter Inputs

In the simulation geometry settings, the design geometry of the draft ship must be in the form of solid bodies. The design geometry and boundary conditions used as space boundaries in the simulation process are shown in Figure 3. The geometrical model of simulation is based on the practical guidelines for ship CFD applications recommended by ITTC (The International Towing Tank Conference). The dimensions used in this geometric model are the overall length, which is twice the length of the ship model, the height of the

inlet and outlet is three times the height of the ship model, the width of the inlet and outlet is three times the width of the ship model.

The simulation has 45778 mesh quality nodes and 199131 elements. The free surface is modeled using the volume of fluid (VoF) method, which involves two phases - water and air. The water conditions are characterized by incompressible flow, as well as steady and multiphase flow. The turbulence model used when water and air fluids are flowing is the k-epsilon standard wall function, which has the simplest turbulence equation. The type of solver chosen is pressure-based because the simulated fluid flow has incompressible flow characteristics. Setting the setup menu in the simulation model includes determining multiphase and turbulence equation models, defining boundary conditions, cell zone conditions, and solution methods.

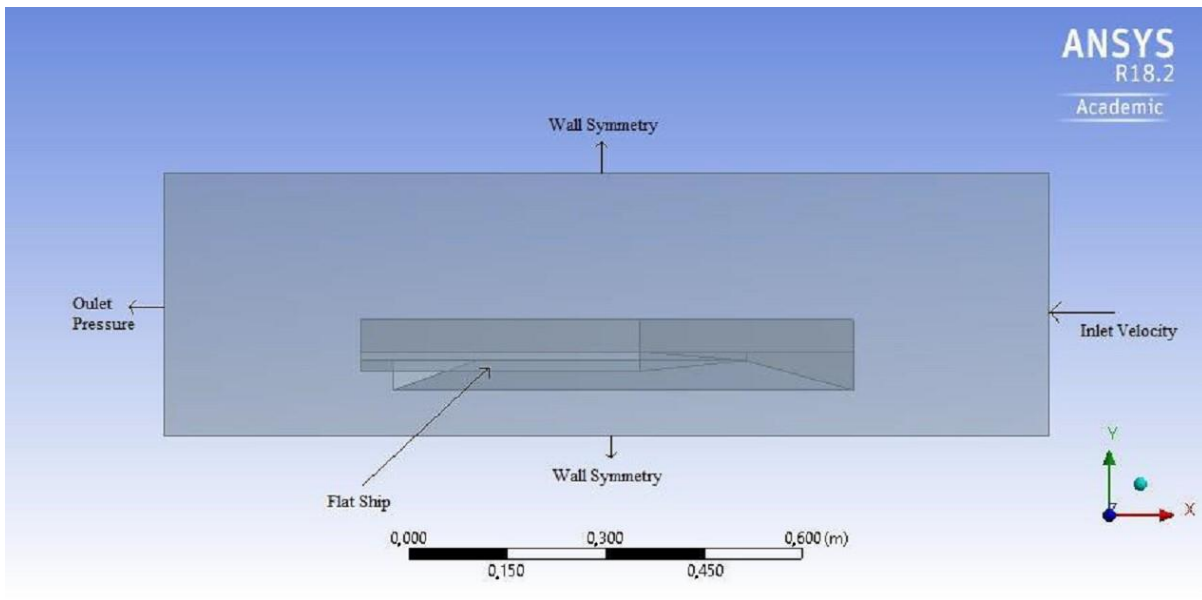


**Figure 3** Boundary conditions on a fast patrol boat simulation

In determining the multiphase model, there are three types of multiphase modeling in Ansys US software (Ansys, 2020), namely Eulerian, VoF, and Mixture. VoF modeling of two phases with a special free surface by tracing the grid mesh that has been made. Meanwhile, the mixture is a two-phase model that is commonly used to model a mixture of two or more fluids. In this study, the VOF model was utilized to model the interface between water and air. A surface tension value of 0.072 N/m was assigned to the water-air interface.

Turbulent fluid flow will tend to occur when a ship passes through the fluid. However, in this case, the flowing fluid is considered a steady flow, and the ship speed is constant so turbulence is predicted to occur, which is not too complicated. Therefore, the K-Epsilon turbulence model is used. In this study, the fluid flow is assumed to be incompressible, viscous, turbulent, and two-phase. Such flow is governed by the incompressible Reynolds-Average Navier Stokes (RANS) equation. The RANS equation has the same general form as the Navier-Stokes equation with velocity and other solutions (Khazaei, Rahmansetayesh, and Hajizadeh, 2019).

The initial state of the geometry and boundary conditions that have been determined will affect the completion of the Navier-Stokes equation and the continuity equation in the simulation process. Boundary conditions are used to model a phenomenon to direct flow in the domain. For flow simulation, boundary conditions are defined as inlet velocity and outlet pressure. There are several different types for certain conditions. In incompressible fluid flow conditions, velocity inlet and outflow are usually used, whereas incompressible

fluid flow conditions, mass flow inlet and pressure far-field are used. However, the selection of boundary conditions can be adjusted to a particular problem model.

In the flow simulation that will be carried out, the model ship, which is called the Hard-chine hull is considered as a static object flowing fluid with the speed variations determined in this study. The inlet of the fluid flow is defined as the velocity-inlet, and the exit area is defined as the pressure-outlet. At the inlet side of the fluid flow, a constant velocity in one direction with a turbulence intensity of 0.5% is considered based on wind tunnel experiments where the inlet turbulent intensity is around 0.5% - 1%. The open channel method, particularly suitable for these conditions, is designated as velocity-inlet. Meanwhile, on the exit side, where the fluid flow maintains a constant static pressure, it is deemed appropriate to define it as a pressure outlet, allowing for the distribution of radial equilibrium pressure. In addition, the bottom side, top side, right side and left side of the domain are defined as walls without friction as a symmetry so that they are considered infinitely wide free surfaces.

The following are the settings used for the boundary inlet and outlet. The inlet is defined as a velocity inlet because, in this simulation, the air and water flow from the inlet at a constant velocity. The input speed for the hard-chine hull model without duct vane is 0.8 m/s, 1.2 m/s, 1.6 m/s, 2.0 m/s, 2.4 m/s, 2.8 m/s and 3.2 m/s. As for the hard-chine hull model with duct vane are 1.6 m/s, 1.9 m/s, 2.2 m/s, 2.4 m/s, 2.7 m/s, 2.9 m/s and 3.2 m/s. The speed variation is considered the Froude number for high-speed patrol boats, and the value is higher than 0.5. The intensity and viscosity of the turbulence are given a small value, namely 0.5%. This aims to minimize the turbulent flow that occurs at the inlet to model calm waters. In the multiphase menu, the flowing fluids are defined as water and air. The free surface level setting is adjusted to the modelling of water depth and ship draft, which is 0.049 m (ship draft). Detailed settings at the inlet and outlet are described in Table 1.

**Table 1** Detail setting of inlet and outlet of the simulation model

Inlet Setting		Outlet Setting	
Reference Frame	Absolute	Backflow Direction Method	Normal to Boundary
Averaged Flow (m/s)	0.8	Backflow Pressure Spec.	Total Pressure
Turbulent Intensity (%)	0.5	Turbulent Intensity (%)	0.5
Turbulent Viscosity	0.5	Backflow Turbulent Ratio	0.5
Multiphase	Open Channel	Multiphase	Open Channel
Secondary Phase	Water	Pressure Specification	Free Surface Level
Free Surface Level (m)	0.049	Bottom Level (m)	0

The Solution Method used in this study was determined based on the validation results. In the validation stage, the least square cell-based method is used. According to the validation results, it was found that the arrangement using the least square cell-based method approached the experimental results with an error percentage of around 1.8%. Pressure velocity coupling is an equation derived from the continuity equation to reduce unexpected pressure conditions. Some of the types are Simple, Simplec, Piso, Coupled, and Fractional Step. In this research, the SIMPLE scheme is used because this scheme considers pressure and speed in its calculations (Patankar, 2018). While the second order upwind on momentum, turbulent kinetic energy and turbulent dissipation rate aim to increase the accuracy of the simulation results. The volume fraction is modeled with compressive characteristics to effectively separate the transition between water and air, facilitated by the surface tension of the water-free surface. The Solution Control parameters used in this study were also determined based on the validation results. According to the results of the validation carried out, the parameters used in the Solution Control settings are obtained as shown in Table 1.

2.3. Validation of Simulation Results

Validation at this stage aims to prove that the results of research data from CFD simulations resemble the results of observational data in experimental tests. It is hoped that the results of the CFD simulation in the form of a graph of velocity against total resistance will have a curve that resembles the graph of velocity against total resistance as the result of the experiment. Table 4 and Table 5 provide a comparison of the results and graphs obtained from experimental testing and CFD simulation for the patrol boat. The results for the patrol boat without a duct vane are shown in Figure 4, while the results for the patrol boat with a duct vane can be found in Figure 5. Validation is carried out by comparing the simulation results with the results of experiments that have been carried out previously. The experiments use the same model dimension as the simulations carried out in the experimental basin. Experiments were carried out with towing tests with the same load and speed variations. The accuracy of the experiment was evaluated using uncertainty analysis. Based on the calculation results of the average deviation error. Obtained error validation results of 2.38%. Because the error obtained is below 10%, it is assumed to be in good agreement. The geometry, mesh, and set-up settings can be used to simulate the Hard-chine hull Ship model. Based on the calculation results of the average deviation error. The obtained error validation results of 3.5%. Because the error obtained is below 10%, the geometry, mesh, and set-up settings can be used to simulate a Hard-chine hull model with duct vane (Duct vane).

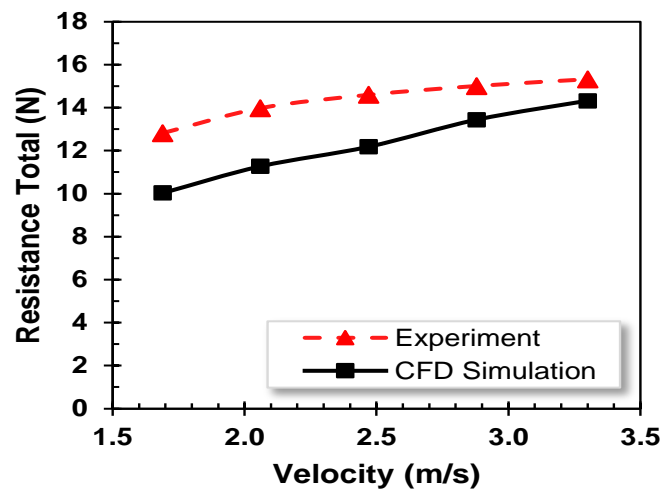


Figure 4 Comparison of total resistance between CFD simulation and experiments without duct vane

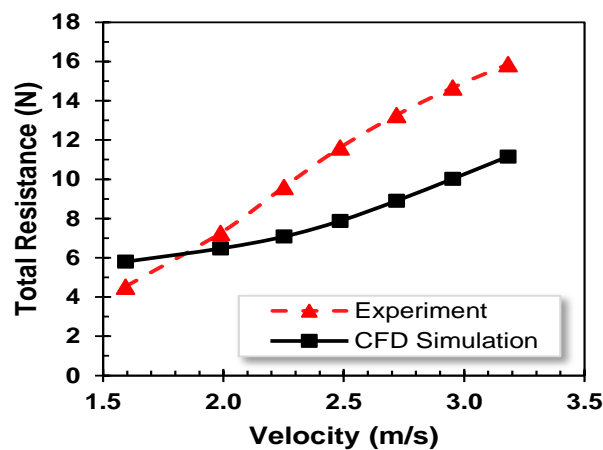


Figure 5 Comparison of total resistance between CFD simulation and experiments with duct vane

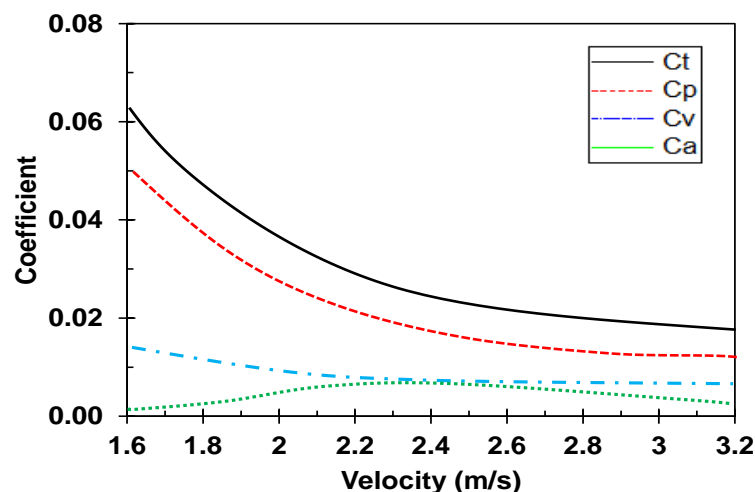
### 3. Result and Discussions

#### 3.1. Comparison of Drag Coefficient

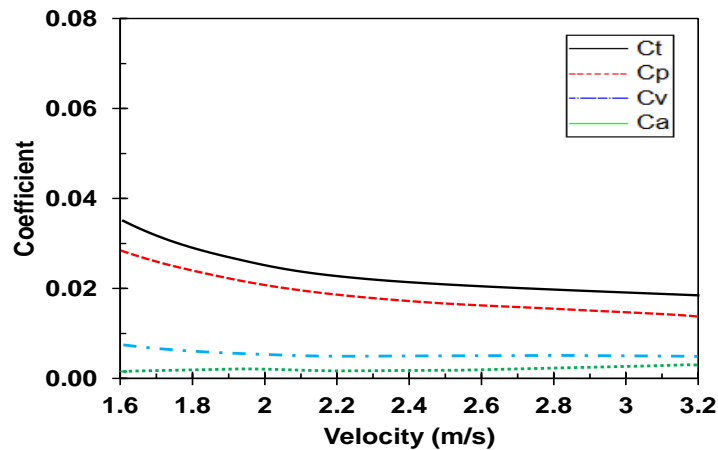
The analysis was carried out to determine the value of the drag coefficient found in Hard-chine hulls without duct vane. The components contained in the total resistance coefficient are the pressure resistance coefficient ( $C_p$ ), the viscous resistance coefficient ( $C_v$ ) and the air resistance coefficient ( $C_a$ ). Figure 6 illustrates the coefficient of viscous resistance, represented by the blue dots, which tends not to experience a significant decrease in the velocity range of 1.6 m/s to 2.2 m/s. In contrast to the coefficient of pressure resistance, which is depicted with red dots, there is a drastic decrease in the velocity range. In this case, it is suspected that the resistance found on Hard-chine hulls without duct vane is dominated by pressure resistance. This is also evidenced by the value of the drag coefficient. In addition, at a velocity range above 3 m/s, the values of the three drag coefficients are getting smaller, and the values of the three are getting closer. This result consistent with the experiment results (Budyanto *et al.*, 2021).

Figure 7 shows the value of the drag coefficient found on a hard-chine hull with a duct vane (Ductship). The main components contained in the total resistance coefficient ( $C_t$ ) are the pressure resistance coefficient ( $C_p$ ), the viscous resistance coefficient ( $C_v$ ), and the air resistance coefficient ( $C_a$ ). As can be seen from the graph below, the pressure resistance coefficient ( $C_p$ ) has the greatest value compared to the viscous resistance coefficient ( $C_v$ ) and air resistance coefficient ( $C_a$ ). In Ductship, the increase in velocity does not significantly affect the magnitude of the viscous drag coefficient ( $C_v$ ). However, the pressure resistance coefficient ( $C_p$ ) value decreases as the velocity value increases.

In comparing the velocity graph to the total resistance ( $R_t$ ) and the velocity graph to the total resistance coefficient ( $C_t$ ), two curves are used, which are the results of the CFD simulation that has been carried out. Figure 8 illustrates the total resistance results for the two model ships. Both curves share a similar shape, indicating that the ship's resistance value increases as the ship's speed rises. The total resistance curve for a flat plate vessel with a duct vane, which is illustrated with a black line, is shown below the total resistance curve for a flat plate vessel without a duct vane of the hard-chine hull, which is colored in red. This proves that the addition of a duct vane on a hard-chine hull can reduce the value of the total resistance on a hard-chine hull. This result is consistence with the previous result (Murdianto, Budyanto, and Syahrudin, 2020).



**Figure 6** Drag coefficient value of hard-chine hull



**Figure 7** Drag coefficient value of application of duct vane

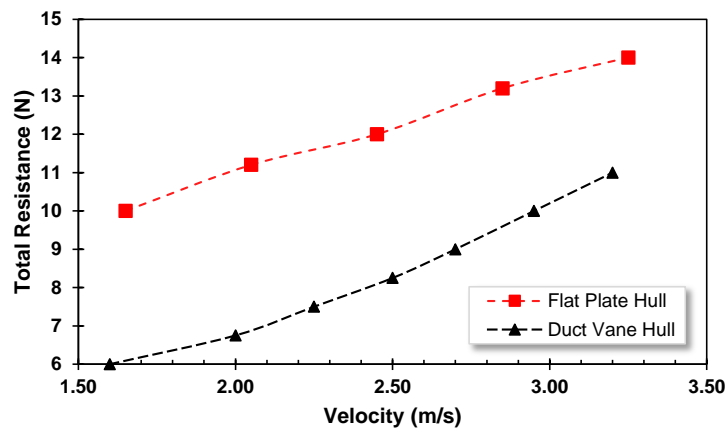


**Figure 8** Comparison of the total resistance of the application of the duct vane

From the results of the comparison of the total resistance, it can be seen that a hard-chine hull with duct vane has a smaller resistance compared to a hard-chine hull without using duct vane (hard-chine hull). At the Froude number ( $F_n$ ) of 0.6, there was a 40% reduction in total resistance (RT). Similarly, at  $F_n$  0.8, there was a 38% reduction, at  $F_n$  0.96, a 30% reduction, and at  $F_n$  1.1, a 20% reduction in total resistance. Observing the calculations of total resistance reduction, it becomes evident that the percentage reduction in total resistance tends to decrease with an increase in speed and Froude number. This proves that the use of duct vane on a hard-chine hull has a percentage reduction in the largest total resistance value at the range of range Froude number of 0.6 to 0.8. In addition to the value of the total resistance of the ship, the coefficient value of the total resistance of the ship is also compared to obtaining a multiplier factor that can be used as a reference to ship design.

### 3.2. Duct Vane Lift Force Analysis

In the previous discussion it was found that the addition of Duct Vane can reduce the total resistance of Hard-chine hulls. This reduction in total resistance is thought to be due to the lift force exerted by the Duct Vane on the stern of the ship. Duct vane is an additional device at the stern of the ship that utilizes the shape of the hydrofoil to generate lift force at the stern of the ship. Based on research conducted through experimental methods, it is known that the shape of the hard-chine hull model tends to experience trim by stern when sailing at high speed. Trim by stern is the condition of the ship when sailing where the stern draft is greater than the bow draft. The addition of a duct vane at the stern of a hard-chine hull can solve the trim problem with the lift force provided by the hydrofoil. As stated in the



discussion chapter on the hydrofoil, the lift force exerted by the hydrofoil is due to the difference in pressure on the hydrofoil cross-section. So at a certain speed, the ship's hull will rise above sea level due to the lift force provided by the hydrofoil (Kandasamy *et al.*, 2011).

The phenomena obtained from the experiments were also proven by the results of the CFD simulations that had been carried out. Figure 9 is the result of a CFD simulation in the form of volume rendering in the form of a pressure contour on the fluid around the simulated model ship. Volume rendering is done when the ship is flowing with fluid at a speed of 1.6 m/s on both ship models. This speed is used because the speed of the model is a speed value that has a significant effect on the difference in resistance. From the results of this volume rendering, it can be seen that the pressure distribution in the fluid around the model ship. Thus, the effect of the addition of Duct Vane on the pressure distribution around the model ship can be analyzed.

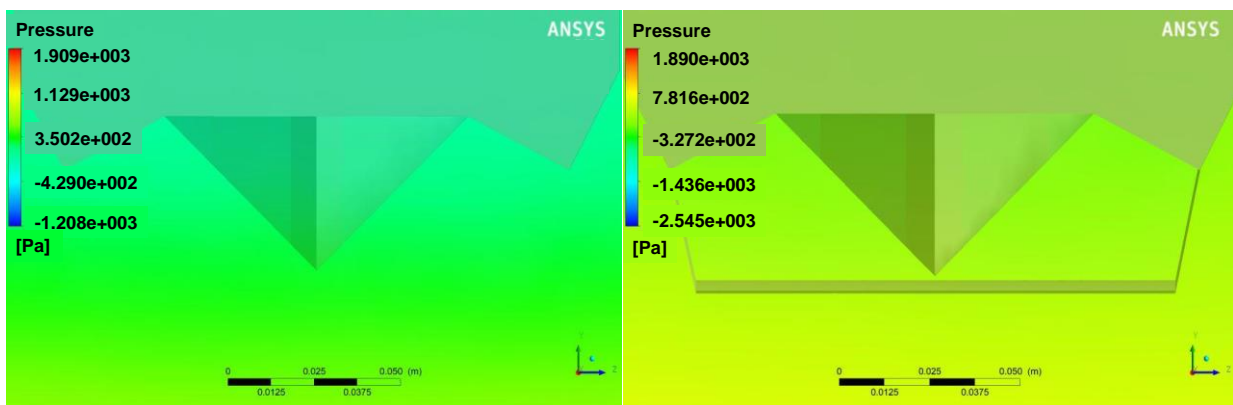


**Figure 9** CFD simulation of a pressure contour on the fluid around the stern hull

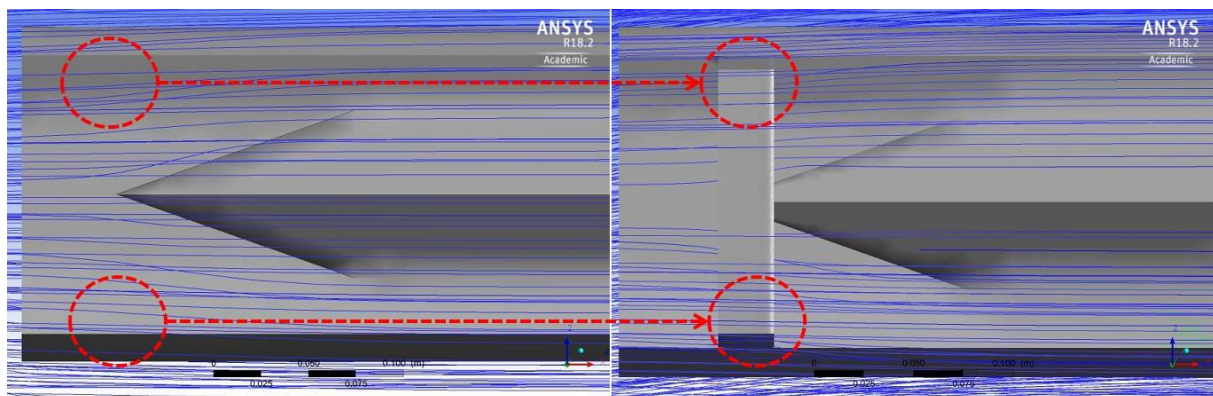


**Figure 10** Fluid flow passes through the stern of the hard-chine hull and duct vane

Figure 10 shows the fluid flow passing through the stern of the hard-chine hull and duct vane. Based on the figure, it can be seen that the flow passing through the stern of a Hard-chine hull without a duct vane has an irregular and inhomogeneous flow direction. It can be seen that several flow lines have different directions. Meanwhile, at the stern of a hard-chine hull with a duct vane, it can be seen that the direction of fluid flow is more homogeneous. The more homogeneous flow is thought to be due to the addition of a Duct Vane at the stern of the hard-chine hull. With a more homogeneous form of fluid flow, the flow separation that occurs at the stern of the ship can be reduced by adding duct vanes to Hard-chine hulls. The shape of the water fluid flow, which is more regular and homogeneous, also affects the value of the pressure resistance and frictional resistance of flat plate vessels. The results of the flow contours show that the addition of a duct vane can

reduce the value of the pressure resistance on hard-chine hulls. One of the additional components of pressure resistance is eddy-making resistance. Eddy-making resistance is an obstacle caused by the separation of shapes on the ship, in this case, on the stern of a hard-chine hull where there are fractures that cause the flow to break away and then form eddies. The addition of duct vane makes the flow at the stern of hard-chine hulls more regular, has a homogeneous direction, and fewer eddies occur compared to the hard-chine hull model, where more eddies occur (Harwood *et al.*, 2019).

#### 4. Conclusions

CFD simulations have been carried out on hard-chine hulls with duct vanes to calculate ship resistance and are validated by experimental test results. The simulation method uses the multiphase volume of fluid equation and k-epsilon as the turbulence equation. Data validation of the simulation results was carried out on experimental results regarding hard-chine hulls with duct vanes. The average deviation error obtained in the validation is around 2-3% for both ship models. From the two simulated ship models, namely hard-chine hulls without duct vanes and hard-chine hulls with duct vanes (ductship), it can be concluded that adding duct vanes to hard-chine hulls can reduce the total drag on hard-chine hulls. The addition of a duct vane on a hard-chine hull can reduce the total resistance of the ship by 40% at  $F_n$  0.6. Suggestions that can be considered for further research development are the collection of experimental data at high speeds to obtain the physical effects due to the lift force from the duct vane.

#### Acknowledgments

The authors express their gratitude to the Faculty Engineering Universitas Indonesia for the Seed Funding Program 2023 number NKB-2563/UN2.F4.D/PPM.00.00/2023.

#### References

- AirfoilTools.com. (n.d.). NACA 4412. Available Online at <http://airfoiltools.com/airfoil/naca4digit?MNaca4DigitForm%5Bcamber%5D=4&MNaca4D>. Accessed on January 22, 2024
- Ansys, 2020. Ansys Fluent: Fluid Simulation Software. © ANSYS, Inc. All rights reserved
- Baso, S., Ardianti, A., Anggriani, A.D.E., Rosmani, R., Bochary, L., 2022. Experimental Investigation of Added Resistance of a Ship using a Hydroelastic Body in Waves. *International Journal of Technology*. Volume 13(2), pp. 332–344
- Budiyanto, M.A., Syahrudin, M.F., Murdianto, M.A., 2020. Investigation of the Effectiveness of a Stern Foil on a Patrol Boat by Experiment and Simulation. *Cogent Engineering*, Volume 7(1), p. 1716925
- Budiyanto, M.A., Murdianto, M.A., Syahrudin, M.F., 2020a. Study on the Resistance Reduction on High-Speed Vessel by Application of Stern Foil Using CFD Simulation. *CFD Letters*, Volume 12(4), pp. 35–42
- Budiyanto, M.A., Wibowo, H.T., Naufal, F., Obindias, R., 2021. Study on the Effectiveness of a Stern-Foil on a Multi-Chine Hulls. *In: IOP Conference Series: Materials Science and Engineering*, Volume 1034, 2nd International Conference on Mechanical Engineering Research and Application, Malang, Indonesia
- Çelik, F., 2007. A Numerical Study for Effectiveness of a Wake Equalizing Duct. *Ocean Engineering*, Volume 34(16), pp. 2138–2145
- Daskovsky, M., 2000. The Hydrofoil in Surface Proximity, Theory and Experiment. *Ocean Engineering*, Volume 27(10), pp. 1129–1159

- Dawangi, I.D., Budiyanto, M.A., 2021. Ship Energy Efficiency Management Plan Development Using Machine Learning: Case Study of CO<sub>2</sub> Emissions of Ship Activities at Container Port. *International Journal of Technology*. Volume 12(5), pp. 1048–1057
- Duy, T.N., Nguyen, V.T., Phan, T.H., Hwang, H.S., Park, W.G., 2022. Numerical Analysis of Ventilated Cavitating Flow Around an Axisymmetric Object with Different Discharged Temperature Conditions. *International Journal of Heat and Mass Transfer*, Volume 197, p. 123338
- Furcas, F., Vernengo, G., Villa, D., Gaggero, S., 2020. Design of Wake Equalizing Ducts using RANSE-based SBDO. *Applied Ocean Research*, Volume 97, p. 102087
- Go, J.S., Yoon, H.S., Jung, J.H., 2017. Effects of a Duct Before a Propeller on Propulsion Performance. *Ocean Engineering*, Volume 136, pp. 54–66
- Harwood, C.M., Felli, M., Falchi, M., Ceccio, S.L., Young, Y.L., 2019. The Hydroelastic Response of a Surface-Piercing Hydrofoil in Multiphase Flows. *Journal of Fluid Mechanics*, Volume 881, pp. 313–364
- Kandasamy, M., Ooi, S.K., Carrica, P., Stern, F., Campana, E.F., Peri, D., Osborne, P., Cote, J., Macdonald, N., Waal, N.d., 2011. CFD Validation Studies for a High-Speed Foil-Assisted Semi-Planing Catamaran. *Journal of Marine Science and Technology*, Volume 16(2), pp. 157–167
- Khazaee, R., Rahmansetayesh, M.A., Hajizadeh, S., 2019. Hydrodynamic Evaluation of a Planing Hull in Calm Water Using RANS and Savitsky's Method. *Ocean Engineering*, Volume 187, p. 106221
- Kim, S., Kinnas, S.A., 2022. A Panel Method for the Prediction of Unsteady Performance of Ducted Propellers in Ship Behind Condition. *Ocean Engineering*, Volume 246, p. 110582
- Köksal, Ç.S., Usta, O., Aktas, B., Atlar, M., Korkut, E., 2021a. Numerical Prediction of Cavitation Erosion to Investigate the Effect of Wake on Marine Propellers. *Ocean Engineering*, Volume 239, p. 109820
- Korkut, E., 2006. A Case Study for the Effect of a Flow Improvement Device (A Partial Wake Equalizing Duct) On Ship Powering Characteristics. *Ocean Engineering*, Volume 33(2), pp. 205–218
- Maxsurf. (n.d.), Intact and Damage Stability Analysis. <https://maxsurf.net/stability> Accessed on 22<sup>nd</sup> January 2024
- Murdianto, M.A., Budiyanto, M.A., Syahrudin, M.F., 2020. Application Of Stern Foil on Full Draft Patrol Vessel at High Speed Condition Using Computational Fluid Dynamics (CFD) Method. *AIP Conference Proceedings*, Volume 2255, p. 020023
- Patankar, S.v., 2018. *Numerical Heat Transfer and Fluid Flow*. CRC Press
- Rezaei, S., Bamdadinejad, M., Ghassemi, H., 2022. Numerical Simulations of the Hydrodynamic Performance of the Propeller with Wake Equalizing Duct Behind the Ship. *Scientia Iranica*, Volume 29(5), pp. 2332–2348
- Riyadi, S., Aryawan, W.D., Utama, I.K.A.P., 2022. Experimental and Computational Fluid Dynamics Investigations into the Effect of Loading Condition on Resistance of Hard-Chine Semi Planning Crew Boat. *International Journal of Technology*. Volume 13(3), pp. 518–532
- Seo, J., Yoon, H.S., Kim, M.il., 2022. Flow Characteristics and Performance of the Propulsion System with Wavy Duct. *Ocean Engineering*, Volume 257, p. 111727
- Syahrudin, M.F., Budiyanto, M.A. and Murdianto, M.A., 2020. Analysis of the Use of Stern Foil on the High-Speed Patrol Boat on Full Draft Condition. *Evergreen*, Volume 7(2), pp. 262–267

- Tacar, Z., Sasaki, N., Atlar, M., Korkut, E., 2020. An Investigation into Effects of Gate Rudder® System on Ship Performance as a Novel Energy-Saving and Manoeuvring Device. *Ocean Engineering*, Volume 218, p. 108250
- Vellinga, R., 2009. *Hydrofoils Design Built Fly*. Peacock Hill Publishing
- Wu, P.C., Chang, C.W., Huang, Y.C., 2022. Design of Energy-Saving Duct for JBC to Reduce Ship Resistance by CFD Method. *Energies*, Volume 15(17), p. 6484
- Yusvika, M., Prabowo, A.R., Tjahjana, D.D.D.P., Sohn, J.M. 2020. Cavitation Prediction of Ship Propeller Based on Temperature and Fluid Properties of Water. *Journal of Marine Science and Engineering*, Volume 8, p. 465